Study and Implementation of Active Noise Control Systems for Magnetic Resonance Imaging

Capstone Report

Aktilek Skakova

Nazarbayev University
Department of Electrical and Computer Engineering
School of Engineering and Digital Sciences

This project report was created on TexStudio editing platform using LaTeX. All the figures were drawn using draw.io online software tool.

NAZARBAYEV UNIVERSITY

Electrical and Computer Engineering
Nazarbayev University
http://www.nu.edu.kz

Title:
Design and Implementation of Active Noise Control Systems for Magnetic Resonance Imaging

Theme:
Theme

Project Period:
Fall 2023 - Spring 2024

Project Group:
Applications of Signal Processing laboratory (ASP-LAB)

Participant(s):
Aktilek Skakova

Supervisor(s):
Muhammad Tahir Akhtar

Copies: 1

Page Numbers: 33

Date of Completion:
May 1, 2024

Abstract:

The objective of the Capstone Project is to study and implement the technique called Active Noise Control (ANC). The project aims to develop an effective ANC system for biomedical applications, namely Magnetic Resonance Imaging to reduce the noise levels generated during the imaging process. The project involved a combination of theoretical study, modeling and simulation. The Benchmark ANC algorithms (Filtered x-Least Mean square (FxLMS), Filtered x-Normalized Least Mean square (FxNLMS) and Filtered x-Variable Step-Size Least Mean square (FxVSSLMS)) were studied to further compare their effectiveness in terms of the steady-state performance, convergence rate and computational complexities based on the computer simulations.

Contents

Dedication vii

Preface viii

Acknowlegment ix

List of Figures x

List of Tables xii

1 Introduction 1
- 1.1 State-of-the-art and related works. . . . 2
- 1.2 Motivation. . . . 3
- 1.3 Capstone Report Organization. . . . 4

2 Fundamental Algorithms and Techniques 5
- 2.1 FxLMS algorithm 6
- 2.2 FxNLMS algorithm 7
- 2.3 FxVSSLMS algorithm 8
- 2.4 Computational Complexity 8
- 2.5 Secondary Path Modelling Techniques 9
  - 2.5.1 Errikson's Method 10
  - 2.5.2 Akhtar's Method 11
- 2.6 Signal Decomposition 12

3 Results and Discussions 15
- 3.1 FxLMS based ANC 15
  - 3.1.1 Acoustic paths 15
  - 3.1.2 Periodic nature of MRI Sound 16
  - 3.1.3 Effect of Step-size paramater 18
  - 3.1.4 Effect of Realization Number 19
  - 3.1.5 Effect of Noise Variance 20

3.1.6 Experimental Results for FxLMS 21
3.2 Simulations for Online Secondary Path Modelling techniques 23
3.3 Performance Comparisons of Benchmark Algorithms 26
3.3.1 FxNLMS algorithm simulations 26
3.3.2 FxVSSLMS algorithm simulations 26
3.3.3 Quantative Results 27

4 Conclusion **29**
4.1 Summary of Work Done 29
4.2 Future work 29

Bibliography **31**

Dedication

This project is dedicated to my family, whose endless support and love has been the driving force behind it. To my dear mother, Bazargul Barankulova, your endless support and the resources you provided were cruical in making this achievement possible. Your faith in me has been a constant source of strength, helping me move forward despite the difficulties.

To my sister Darina Skakova, who looks up to me as a role model, who believed in me from the very beginning, I dedicate this work in the hope that it will inspire you to follow your dreams. Your presence on this journey has been a reminder of the importance of perseverance and determination.

I am deeply grateful to my family for their love, guidance and support. Without their unwavering faith in my abilities, this achievement would not have been possible.

Preface

This project focuses on the development of an Active Noise Control (ANC) system designed for Magnetic Resonance Imaging (MRI) applications which aims to reducing noise levels. This technology contributed the enhancing the quality of MRI scans, and its potential application extends to the field of MRI equipments in Kazakhstan, and can be used worldwide. As ANC technology continues to be involved and integrate into medical imaging, this project can lead to further advancements, including real-time noise reduction, adaptive algorithms for diverse MRI tools, and expanded applications beyond conventional MRI. Effective algorithms with higher performance results can yield valuable ways to combat not only the noise in MRI scans but other biomedical applications that generate noise and disturb the patients to conduct medical procedures.

In Chapter 1, the basis of ANC, its principle and applications in all spheres, also the types of noise generated by MRI are discussed. Chapter 2 covers benchmark algorithms - FxLMS, FxNLMS and FxVSSLMS - detailing the underlying mathematical principles. In addition, methods for decomposing the signal based on features of fMRI audio data are discussed. In Chapter 3, the simulation results for all benchmark algorithms, and secondary path modelling techniques are presented. This is followed by an analysis of the nature of MRI sound. The simulation includes the influence of various parameters on the performance of the algorithms and comparison of benchmark algorithms in terms of performance metrics. The final section presents a comprehensive conclusion that outlines the findings and implications of the main project. This section summarizes the findings from the report and provides a brief overview of the project's contributions to the field and future applications.

Nazarbayev University, May 1, 2024

Aktilek Skakova
<aktilek.skakova@nu.edu.kz>

Acknowledgement

I would like to express my deepest gratitude to the researchers whose contributed to the advancement of active noise control. The publications, papers and books written by Sen M. Kuo, Dennis R. Morgan, S.Haykin, Behrouz F. Boroujeny, I. Pannahi, G. Kannan, A. Ganguly particularly formed the basis of this project.

Under the guidance of my supervisor and esteemed professor, Muhammad Tahir Akhtar, I had the opportunity to conduct my project within the Application of Signal Processing lab. I would like to express my sincere gratitude to Prof. Akhtar, for his support and guidance during my project. His lectures and office hours have significantly shaped my understanding and approach to this field.

I am also thankful to the members of the Application of Signal Processing lab for their collaboration, knowledge sharing, and constructive feedback. The weekly seminars provided an invaluable oportunity for exchanging ideas, discussing challenges, and tracking our progress.

List of Figures

1.1 The illustration of the principle of ANC 2

2.1 Detail of Implementation of the ANC system [15] 6
2.2 The block scheme implementation of Eriksson's technique based ANC System [25] 10
2.3 The block scheme implementation of Akhtar's technique based ANC System [26] 12
2.4 Schematic diagram of FxLMS FANC with signal decomposition [13] 14

3.1 (a) Impulse responce characteristics of secondary path $S(z)$ used in computer simulations, (b) The corresponding magnitude responce characteristics of $S(z)$ 15
3.2 (a) Impulse responce characteristics of secondary path $P(z)$ used in computer simulations, (b) The corresponding magnitude responce characteristics of $P(z)$ 16
3.3 Autocorrelation of recorded MRI sound 16
3.4 Superposition of ten Adjacent Segments of MRI noise 17
3.5 Superposition of ten Adjacent Segments of MRI noise for 30 samples 17
3.6 MSE curve for different step-size parameters 18
3.7 MSE curve for different realization numbers 19
3.8 MSE curve for different SNR values 20
3.9 (a) MSE curve versus number of iterations for tonal signal, (b) Tonal signal $x(n)$ and error signal $e(n)$ versus number of iterations 21
3.10 (a) MSE curve versus number of iterations for broadband bandlimitted signal, (b) Broadband bandlimitted signal $x(n)$ and error signal $e(n)$ versus number of iterations 21
3.11 a) Identification error of Secondary Path modelling b) Coeficients of true and estimated secondary paths 22

3.12 (a) error signal $e(n)$ versus number of iterations for broadband bandlimitted reference signal (b) Input signal $x(n)$ and output signal $y(n)$ versus number of iteration for broadband bandlimitted reference signal 23
3.13 (a) error signal $e(n)$ versus number of iterations for tonal reference signal using Errikson's method (b) Input signal $x(n)$ and output signal $y(n)$ versus number of iteration for tonal reference signal using Errikson's method 24
3.14 Step-Size adapatation for Akhtar's method 25
3.15 (a) error signal $e(n)$ versus number of iterations for broadband bandlimitted reference signal using Akhtar's method (b) Input signal $x(n)$ and output signal $y(n)$ versus number of iteration for broadband bandlimitted reference signal using Akhtar's method 25
3.16 MSE curves for FxLMS and FxNLMS algorithms based ANC system 26
3.17 MSE curves for FxVSSLMS and FxLMS algorithms based ANC system 27

List of Tables

2.1 FxLMS algorithm's computational complexity 9
2.2 FxNLMS algorithm's computational complexity 9
2.3 FxVSSLMS algorithm's computational complexity 9

3.1 Simulation Parameters for FxLMS algorithm 18
3.2 Simulation Parameters for Secondary Path Modelling 23
3.3 NAL values for adaptive algorithms 28

Chapter 1

Introduction

Many medical and heating, ventilation, and air-conditioning (HVAC) technologies generate unwanted noise that disturbs humans and can even be hazardous to their health [1]. Also, with the increase of the large industrial sites, and high-density housing the problem with noises is becoming more and more evident. The traditional approach includes passive noise control where the enlosures, silensers and barriers are used to diminish the undesired noise. This technique uses the principle of the impedance change or uses the energy loss caused by sound propagation of these special materials. However in some cases the use of passive mathods are not efficient in terms of the required cost and ineffictiveness to low frequencies. Therefore, the more research and applications are conducted for Active Noise Control (ANC). ANC is a technique used to cancel or to reduce unwanted noise in a specific environment by generating an opposing sound wave that has the same amplitude but reversed phase which effectively cancels the noise. ANC systems consist of a microphone, a digital signal processor (DSP), and a speaker. The microphone captures the noise, and the DSP analyzes the sound signal to determine its frequency and amplitude characteristics. Then, the DSP generates an inverted sound wave with the same frequency and amplitude as the original noise. The inverted sound wave is played through the speaker, and when it combines with the original sound wave, they destructively interfere with each other, canceling out the noise. ANC is used in many applications, such as noise-canceling headphones, automobiles, airplanes, and other vehicles to cancel out engine noise and other unwanted sounds [2]. One of the frequently used technologies in medicine that generates loud noises is Magnetic resonance imaging (MRI). This is a often used medical imaging technique in radiology to form pictures of the anatomy and the physiological processes of the body. This tool uses a strong magnetic field and radio waves to produce detailed images of the body's internal structures, and as a result generates the loud noise that should be diminished [3]. Therefore, it is important to decrease the sound level of the noise and remove it. Further more the

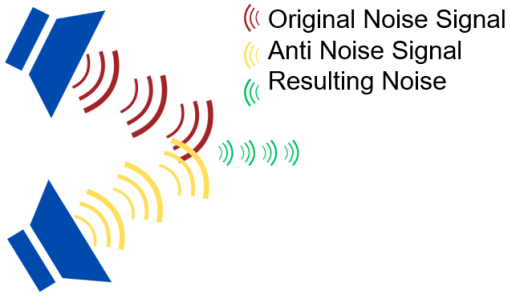

Figure 1.1: The illustration of the principle of ANC

noise generated from fMRI affects the brain activity, which consequenctly lead to the incorrect results of diagnostics [4]. Various methods have been applied to solve this problem, but depending on the characteristics of the noise, the methods may not be effective for all kinds of noise. Therefore, there is a demand for decreasing the noise level at all frequencies, including low-frequency and impulsive noise [5]. The destructive interference principle is depicted in Fig. 1.1. The original noise generated by MRI will be diminished by the anti noise signal that resulted from the ANC system, leading to minimizing the overall noise.

1.1 State-of-the-art and related works.

Noise generated by MRI ranges from 65 dB to 130 dB. Based on the World Health Organization (WHO) data, the sound higher than 70dB is considered as the hazardous for the health of people, even can lead to the hearing loss as a result of the continuous noise [6]. There are various types of the noise are generated from MRI:

- Gradient Noise: Gradient coils that are the core of MRI cause vibrations that generate noise, which can be heard as a banging or knocking sound.
- Mechanical Noise: The MRI scanner's moving parts, such as the cooling fans and pumps, can create mechanical noise. The noise is often described as a humming or buzzing sound.
- Acoustic Noise: The rapid switching of the magnetic fields and the vibration of the gradient coils cause pressure waves in the air, creating acoustic noise. This noise can be as loud as 110 dB.

One type of the acoustic noise is impulsive noise, which is a sudden burst of sound energy that occurs in a very short time frame. This type of noise is typically caused by the rapid switching of magnetic gradients inside the MRI machine, which can create a sharp, loud noise that can be uncomfortable for the patient. The noise can

cause discomfort and anxiety in patients and may also make it difficult for them to communicate with the MRI staff. Feeling anxiety, being scared and not relaxed condition can lead to the not clear and false result of the testing [7].

An adaptive filter is a digital filter that automatically adjusts its coefficients to optimize its output in response to changes in the input signal. It is a system that changes its behavior over time in order to better match the characteristics of the signal it is processing. The main function of it is to minimize the difference between the desired and output signal. So the filter reshapes the input signal to match the desired signal, and the error signal should approach to 0. Adaptive filters are commonly used in signal processing applications such as noise reduction, echo cancellation, equalization, and channel estimation [8]. Discovering the nature of the noise generated by MRI is beneficial to enhance the performance of the overall ANC system, and can lead to better prediction results. The frequency-encoding gradient pulses are encountered more oftern and exhibited generally odd-number harmonics and nonharmonics [9]. The well-established fact is that fMRI acoustic noise, particularly when employing the Echo Planar Imaging (EPI) technique, demonstrates a periodic structure due to the rapid switching of magnetic gradient currents in the scanning coils. Periodicity nature allows to use the linear prediction (LP) filtering techniques to separate the dominant frequency parts from residual ones [10] [11]. The quasi periodic feature of the noise from MRI makes to possible to get rid of the limitation which was created as a result of the non-minimum phase nature of the secondary path. Based on the periodic nature, the equalizing filter can be designed that neutralizes the secondary path [12] [13].

1.2 Motivation.

The aim of this project is to implement the ANC system for MRI based on the existing algorithms. The ANC have been applied for reducing the noise, but the effective design with the higher performance in terms of the noise decrease level for particularly MRI technology was not fully discovered. Therefore, the objective is to develop the suitable algorithm and propose the new algorithm with better results. MRI technologies uses the special headphones which is the method of Passive Noise Control to diminish the unwanted noise, however this technique is effective only for high frequencies. While the noise generated by MRI is both low and high frequencies, also it overlaps with region where the human ear is mostly sensitive. There are only few MRI technologies that integrated with ANC, as the system should not interrupt the main operation of the MRI testing, also requires the additional place and more expensive to implement. Therefore, the project aims to implement the ANC system such that it maximizes efficiency for wide range of noise and will be autonomy with regard to the installation with relative affordable price and the simplicity of the implementation.

1.3 Capstone Report Organization.

The Capstone Report is divided into four main chapters, each designed to provide a comprehensive understanding of the project's goals, methodologies, and results. The first Chapter gives an introduction to ANC, its working mechanism and applications. In Chapter 2, the benchmarks algorithms (FxLMS, FxNLMS and FxVSSLMS) are explained with the mathematics behind them. Chapter 3 covers all simulations done for this project with the analysis. In Chapter 4, the conclusion drawn from the project and the future work that can be done are discussed.

Chapter 2

Fundamental Algorithms and Techniques

Adaptive filtering is a technique used in signal processing to adjust the coefficients of a filter dynamically, based on the input signal characteristics. It's widely employed in various applications such as noise cancellation, equalization, echo cancellation, and channel estimation.

The main idea behind adaptive filtering is to continuously update the filter coefficients to minimize the difference of system's desired output and the true output. This adjustment is done iteratively using adaptive algorithms. The signal degradation on some physical systems is time varying and unknown. Adaptive systems modify their characteristics and adjust coefficients by adaptive algorithms for time-varying system applications. One of the most commonly used algorithmis is Least Mean Square (LMS) algorithm. The pervasive performance is measured based on the mean-square error (MSE):

$$J(n) = E[e^2(n)], \tag{2.1}$$

where $E[]$ denotes expected value.
The LMS algorithm updates the weight vector as follows:

$$w_i(n+1) = w_i(n) + \mu e(n)x(n-i), \tag{2.2}$$

Filtering output:

$$y(n) = \sum_{i=0}^{M-1} w_i(n)x(n-i), \tag{2.3}$$

Error estimation is the difference of the output and desired signals:

$$e(n) = d(n) - y(n), \tag{2.4}$$

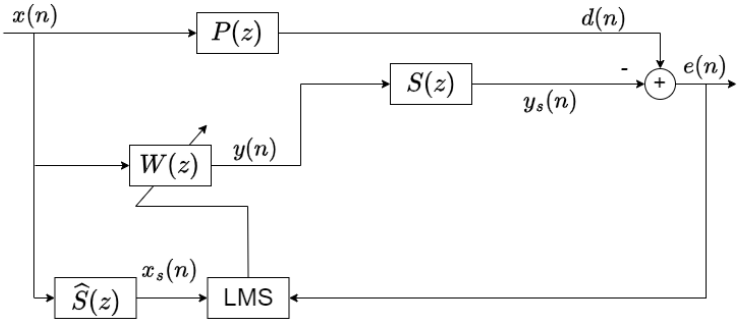

Figure 2.1: Detail of Implementation of the ANC system [15]

Where: $y(n)$ - output signal, $x(n)$ - input signal, $e(n)$ - error signal, $w(n)$ - tap weight coefficient, μ - step size.

The objective is to determine the weight vector so that the mean-square value of the error signal is minimized. This algorithm is simple, also does not require squaring, averaging or differentiating. Furthermore, its expected value of the weight vector converges to the Wiener filter.

ANC is a method that involves the use of a secondary sound to diminish undesired noise, effectively canceling out the initial sound. The diagram representing the ANC system is displayed in Fig. 2.1. $P(z)$ is the primary acoustic path between the reference noise source and the error microphone. The reference noise signal $x(n)$ undergoes filtering via $P(z)$, and this signal is denoted as $d(n)$ which is captured by the error microphone. The adaptive filter $W(z)$ should generate an antinoise signal $y(n)$ propagated by the secondary loudspeaker. These primary and antinoise signals are combined together and create the silent zone near the error microphone. This error microphone measures the difference between the primary noise and the output signal $e(n) = d(n) - y_s(n)$, where $y_s(n) = s(n) * y(n)$, and $s(n)$ is the impulse responce of the secondary path $S(z)$ [14].

2.1 FxLMS algorithm

The secondary path effect is indirect acoustic routes that changes the anti-noise signal's characteristics before it reaches the error microphone, which lead to reducing the effectiveness of noise cancellation. Therefore, it is important to compensate for secondary paths in active noise control. By taking into consideration these acoustic pathways through adaptive algorithms, the system can continuously adjust the anti-noise signal to maintain its effectiveness despite changes in the environment [16]. The conventional LMS alogirthm does not take into account the secondary path effect. This can lead to poor performance of the noise cancellation system. To solve this issue, the modified version of the LMS algorithm called FxLMS is

obtained. FxLMS algorithm uses a filter to model the secondary path by filtering out the input signal. This allows the algorithm to adjust the filter coefficients in response to changes in the secondary path, resulting in better performance and stability of the noise cancellation system [17]. This algorithm requires the knowledge of the transfer function $S(z)$, and it is another scope of the investigation as this estimation can be done by different techniques. Off-line modelling can be used to estimate $S(z)$ during an initial training stage. After the estimation, the model $S'(z)$ is fixed and further will be used for ANC system. The off-line modelling has the severe disadvantages of not adaptively responding to the changes in the secondary path, as it can be continuously changing over the time, and it results in poor estimation. Therefore, the on-line modeling technique is highly preferable [18].

The residual signal is expressed as:

$$e(n) = d(n) - y'(n) = d(n) - s(n) * y(n), \tag{2.5}$$

where $s(n)$ is the impulse responce of the secondary path $S(z)$ at time n.

The FxLMS algorithm updates the weight vector as follows:

$$w_i(n+1) = w_i(n) + \mu e(n) x'(n-i). \tag{2.6}$$

In practical ANC applications, $S(z)$ is should be estimated with an addition filter $S'(z)$. Therefore, the reference signal passing through this estimate of the secondary path can be expressed as:

$$x'(n) = s'(n) * x(n). \tag{2.7}$$

2.2 FxNLMS algorithm

The system stability, the time required for convergence, and robustness depends on the step size parameter of algorithm and the power of reference signal. The conventional LMS algorithm has a low convergence rate.Therefore, to have a better performance, the variants of the LMS algorithm were obtained. Normalized LMS algorithm can be utilized in order to achieve higher speed of convergence ensuring the better steady-state performance.

Step size parameter is defined by the following equation [19]:

$$\mu = \frac{a}{x^T(n)x(n)}, \tag{2.8}$$

where a is a normalized step size that satisfies the criterion

$$0 < a < 2. \tag{2.9}$$

For application of ANC, the secondary path will be taken into account, and resulting FxNLMS algorithm can be expressed as

$$w_i(n+1) = w_i(n) + \mu e(n) x'(n-i). \tag{2.10}$$

Zhang et al. explored the robustness of the FxNLMS algorithm in the presence of input signals with varying power levels and system uncertainties. Their analysis revealed that the FxNLMS algorithm exhibits higher robustness to changes in input signal power, making it well-suited for real-world applications where signal characteristics may fluctuate over time which is the case of fMRI noise nature [20].

2.3 FxVSSLMS algorithm

One of the classes of LMS algorithm is Variable Step-Size LMS (VSSLMS) algorithm, where the step-size parameter changes according to an estimate of the minimum MSE, which results in better convergence rate [21]. It was proven that the use of VSSLMS algorithm increases the computational complexity only to 15 % compared to traditional LMS algorithm, while the convergence time can be decreased two times. The weight vector with filtered input is updated based on the following formula:

$$w_i(n+1) = w_i(n) + U(n) e(n) x'(n-i), \tag{2.11}$$

where $U(n)$ is the diagonal matrix of step-sizes for each time at time n

$$U(n) = \begin{bmatrix} \mu_0(n) & 0 & ... & 0 \\ 0 & \mu_1(n) & 0 & ... \\ ... & ... & ... & 0 \\ 0 & ... & 0 & \mu_{L-1}(n) \end{bmatrix} \tag{2.12}$$

Adjusting the step-size parameter individually for each tap is a commonly used in adaptive algorithms. Initially, employing a larger step-size resulys in higher convergence, facilitating rapid adaptation to changes within the system or environment. Then, to prevent large misadjustment and ensure stability as the algorithm approaches the optimal solution, it's beneficial to gradually reduce the step-size. This adaptive approach not only facilitates rapid convergence but also results in stable performance over time, making it particularly effective in scenarios where system dynamics vary.

2.4 Computational Complexity

One of the main criteria for choosing the algorithm is the computational complexity as it determines the speed and efficiency of real-time noise cancellation processes, enabling rapid analysis and response to incoming sound. Understanding

and minimizing computational complexity in ANC technology allows for scalable and efficient noise cancellation solutions across diverse environments and devices [20]. The following tables show the compuational complexity for three different ANC algorithms.

Table 2.1: FxLMS algorithm's computational complexity

	Equation	Multiplication	Addition
1	$y = w^T(n)x(n)$	L	L-1
2	$e(n) = d(n) - y(n)$	0	1
3	$w(n+1) = w(n) + \mu x'_s(n)e(n)$	L+1	L
4	$x_s(n) = s'(n) * x(n)$	M	M-1
	Total	2L+M+1	2L+M-1

Table 2.2: FxNLMS algorithm's computational complexity

	Equation	Multiplication	Addition
1	y=w^t(n)x(n)	L	L-1
2	e(n)=d(n)-y(n)	0	1
3	w(n+1)=w(n)+mx_s(n)e(n)	L+1	L
4	x(n)=s'(n)*x(n)	M	M-1
5	$\mu(n) = \frac{a}{x^T(n)x(n)}$	L	L-1
	Total	3L+M+1	3L+M-2

Table 2.3: FxVSSLMS algorithm's computational complexity

	Equation	Multiplication	Addition
1	y=w^t(n)x(n)	L	L-1
2	e(n)=d(n)-y(n)	0	1
3	w(n+1)=w(n)+mx_s(n)e(n)	L+1	L
4	x(n)=s'(n)*x(n)	M	M-1
5	$\mu(n)$	L	L-1
	Total	3L+M+1	3L+M-2

2.5 Secondary Path Modelling Techniques

Efficient operation of ANC systems depends on accurately modeling the secondary path, which defines relation of the the input signal to the residual noise. When the secondary path estmation $S'(z)$ has a sufficiently high order, and both the primary

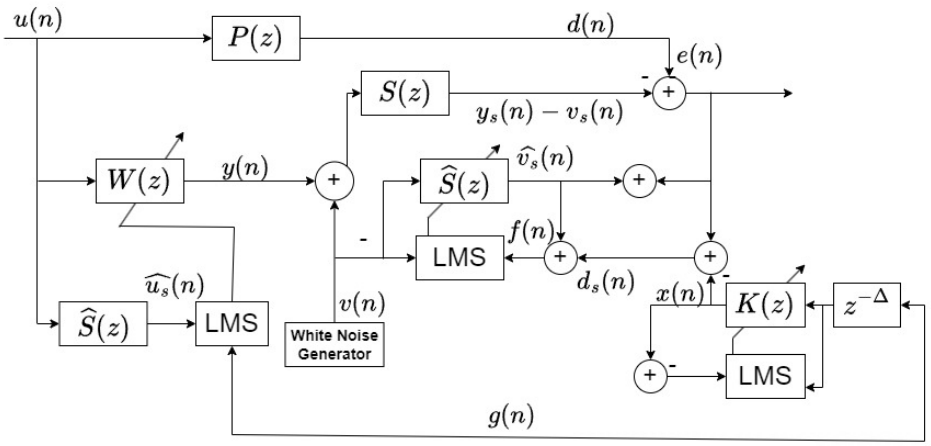

Figure 2.2: The block scheme implementation of Eriksson's technique based ANC System [25]

and secondary paths exhibit changing characteristics over time, the system's stable state can be described by the following equation:

$$S(z) - \widehat{S}'(z) = \frac{P(z)}{W(z)}. \tag{2.13}$$

The estimated secondary path will be the same as the actual secondary path $S(z)$, if the primary path $P(z)$ is zero, which the desired signal $d(n)$ is also zero [22].

The secondary path modelling's accuracy is affected by two factors: first of all $S(z)$ should be estimated independently of control fiter in order to ensure the system's stability, and secondly the estimate should not disturb the ANC system itself. The estimation of $S'(z)$ can be conducted either when ANC is in operstion or offline prior to the operation of ANC. Online estimation of secondary path when the secondary path's characteristics change over time [23].

Modeling the secondary paths can be done through general two main approaches: using additional white noise for system identification or using directly the output of the ANC controller filter to estimate the secondary path. Studies show that the former method, with auxiliary noise, is more efficient in terms of computational complexity, steady-state indicator, and rate of convergence because of the uncorelatedness of the two processes. Hence, the research is mostly focused on the method with additional noise [24].

2.5.1 Errikson's Method

The technique proposed by Eriksson et al. uses an additional noise [25]. An on-line secondary path modelling with additive random noise id depicted in Fig. 2.2. The

random noise generator produces zero-mean white noise, which is not correlated with the primary noise. This signal is then combined with the secondary signal which is the result of the $W(z)$ filter. The residual error can be represented as:

$$e(n) = d(n) - y_s(n) - v_s(n). \tag{2.14}$$

Above used secondary noise resulting from the original noise can be obtained as:

$$y_s(n) = s(n) * y(n). \tag{2.15}$$

The modified noise due to auxiliary noise is defined as

$$v_s(n) = s(n) * v(n). \tag{2.16}$$

The modelling filter $\widehat{S'}(z)$ yields an estimate of Eq.(3)

$$\widehat{v_s}(n) = \widehat{s}(n) * v(n). \tag{2.17}$$

The parameters of the adaptive filter $S'(z)$ are adjusted through conventional LMS algorithms, and defined as:

$$\begin{aligned} \widehat{\boldsymbol{s}}(n+1) = \widehat{\boldsymbol{s}}(n) + \mu_s \boldsymbol{v}(n) f(n) = \\ \widehat{\boldsymbol{s}}(n) + \mu_s \boldsymbol{v}(n)[v_s(n) - \widehat{v_s}(n)] - \mu_s \boldsymbol{v}(n) x(n), \end{aligned} \tag{2.18}$$

where μ_s is the step size for the modelling process, and reference signal vector $\boldsymbol{v}(n) = [v(n)v(n-1)...v(n-L+1)]^T$. The error signal $f(n)$ is utilized to modify secondary path modelling filter. $W(z)$'s coefficients are adjusted based on the FxLMS algorithm:

$$\begin{aligned} \boldsymbol{w_c}(n+1) = \boldsymbol{w_c}(n) + \mu_w g(n) \widehat{\boldsymbol{u_s}}(n) = \\ \boldsymbol{w_c}(n) + \mu_w \widehat{\boldsymbol{u_s}}(n)[d(n) - y_s(n) + \mu_w \ \widehat{\boldsymbol{u_s}}(n) v_s(n), \end{aligned} \tag{2.19}$$

where μ_w is control process step-size, $\widehat{\boldsymbol{u_s}}(n) = [\widehat{u_s}(n)\widehat{u_s}(n-1)...\widehat{u_s}(n-M+1)]^T$, and reference signal $u(n)$ filtered out by S'(z) defined as $\widehat{u_s}(n)$

2.5.2 Akhtar's Method

Eriksson's technique was improved further by various methods discussed in other studies. Bao et al. introduce an extra adaptive filter to mitigate interference stemming from Eriksson's approach and improve convergence speed [26] . However, this doesn't enhance the control filter's performance. Kuo's method also uses one more adaptive filter to predict error signals and eliminate interference effects, but the delay needs optimization to prevent degradation of the overall system performance. Zhang's method additional filter for Eriksson's which is aimed to diminish

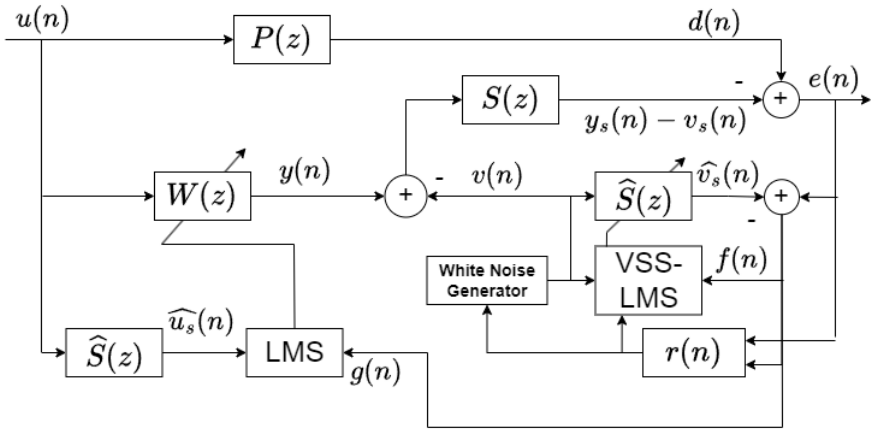

Figure 2.3: The block scheme implementation of Akhtar's technique based ANC System [26]

the interference caused by other filters. The method proposed by Akhtar uses Variable Step size algorithm that adjusts the step-size parameter based on the system's convergence, and this method outperforms mentioned methods by reducing disturbance caused by white noise signals [27] [28]. The ANC with Secondary modelling based on Akhtar's method is illustrated in Fig. 2.3 The ratio of the power of residual and modelling errors $P_e(n)$ and $P_f(n)$ correspondingly determines the step-size parameter. The ratio is defined by the following formula:

$$r(n) = \frac{P_f(n)}{P_e(n)}, \tag{2.20}$$

where the formula for power can be obtained as:

$$P_x(n) = (1-\lambda)e^2(n) + \lambda P_x(n-1), \tag{2.21}$$

where λ is a forgetting factor and can be chosen within the range of 0.9-1.0.

Then, this ratio is used to update step-size for each iteration by the formula defined as:

$$\mu_s(n) = (1 - r(n))\mu_{s_{\max}} + r(n)\mu_{s_{\min}}. \tag{2.22}$$

The limits of the step-sizes can be empirically obtained by the stability curve of the system. Auxilliary noise is also employed, and then the proposed VSS-LMS algorithm is applied to estimate the secondary path while ANC in operation based on the FxLMS algorithm.

2.6 Signal Decomposition

It was proven that fMRI noise exhibits high degree of periodicity due to the rapidly switched magnetic magnetic gradient currents in the coils [11] [29]. Use of this

feature of the fMRI noise can give higher performance. Based on the Wold decomposition theorem all stochastic processes can be can be splitted into dominant periodic and residual aperiodic components. By using this theorem, it is preferable to first decompose the signal into predictable and random part with the help of linear prediction (LP) filtering. The LP filtering is easier and has less computational complexity compared to other methods [30].

The first step of the decomposition with the noisy input error signal involves temporal feature analysis, where the autocorrelation sequence is computed using an appropriate length of data samples. As a result, the period N can be found based on the periodicity property of the autocorrelation sequence of the periodic signal [13]. This N period will futher used as the order of the LP filter. The main objective of the signal decomposition is to decompose the signal into two parts: one with the dominant frequency, and resudual frequency components. Consider the error signal $e(n)$ in the following form [31]:

$$e(n) = e_p(n) + e_w(n) \tag{2.23}$$

where: $e_p(n)$ is the periodic part of the error signal, while $e_w(n)$ is remaining part.

The next step involves the spectral feature estimation to determing LP filter coefficients. Then by the peak detection will implied as the frequency at which each peak occurs corresponds to one of the individual frequencies ω_k. For each detected peak in the magnitude spectrum,frequency ω_k, amplitude A_k and phase θ_k will be extracted. The estimate of the periodic signal $e_p(n)$ can be constructed by summing up these individual components at each peaks. The aperiodic part can be found by substracting this periodic part from the overall error signal $e(n)$. Once the signal is separated, active noise control for each component will applied separately and effectively. The decomposition of the signal is finished by utilizing a specialized NLMS adaptive filter, aiming to synchronize the phase of $e_p(n)$ with $e(n)$. The following figure shows the block scheme implementation of the overall system: As depicted in Fig. 2.4, the proposed system to manage fMRI acoustic noise involves a sequential process: (1) Signal decomposition, (2) Signal synchronization, and (3) Active noise control based on FxLMS adaptive algorithm. Implemented within a FANC architecture, the system operates solely on the error signal from the microphone, $e(n)$. As there is no access to the reference signal the adaptive algorithm should estimate the reference noise using the error signal, which make the adaptive FANC systems more complex and computationally challenging for real-time implementation [13].

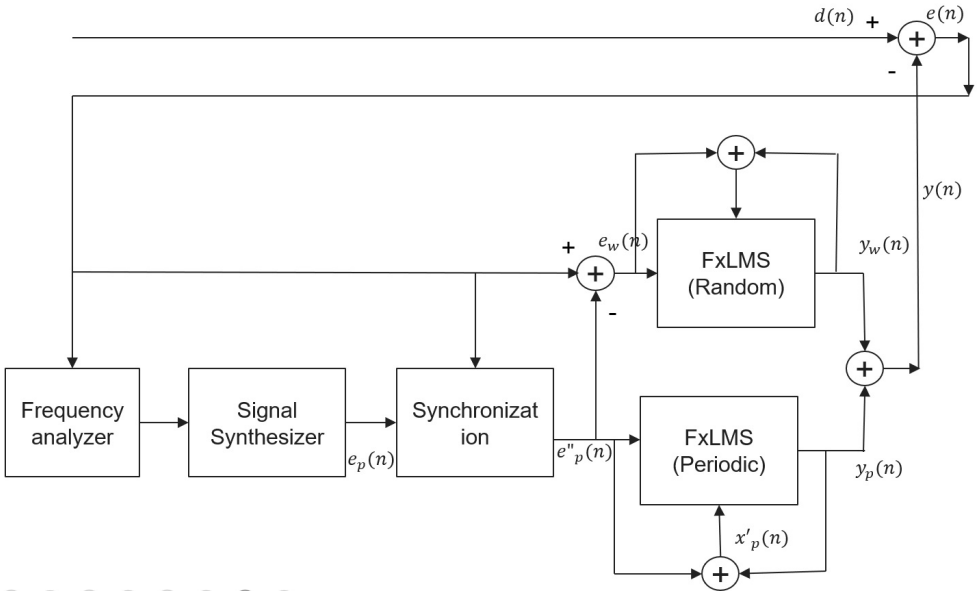

Figure 2.4: Schematic diagram of FxLMS FANC with signal decomposition [13]

Chapter 3

Results and Discussions

3.1 FxLMS based ANC

3.1.1 Acoustic paths

The simulations for ANC algorithms were carried out using the estimated of the acoustic paths.The first task in active noise control involves estimating the impulse response of the secondary and primary propagation paths. These approximation models are beneficial for project goals of comparing various algorithms performance within identical conditions. The models were obtained as linear causal stable single-input single-output transfer functions, $P(z)$ and $S(z)$ The secondary path impulse response is generated by computer using the filter with the sampling frequency of 8kHz, and their corresponding frequency responces are given in Fig. 3.1 generated by filter bandlimited to the range 200 - 800 Hz with a length of 0.1 seconds.

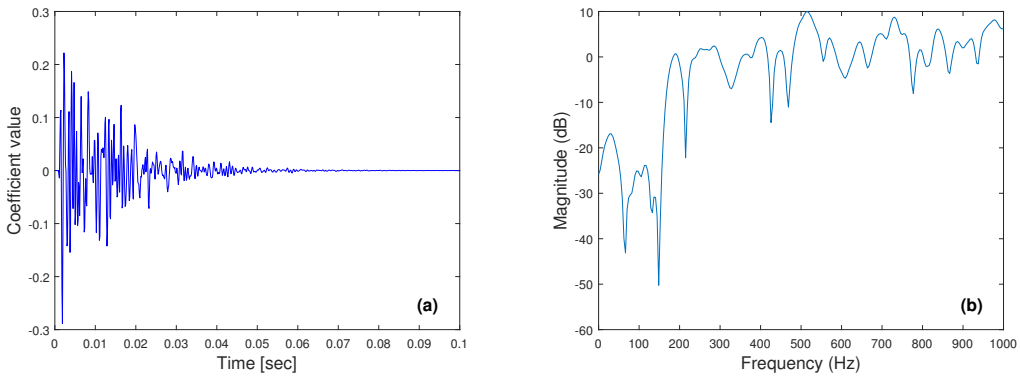

Figure 3.1: (a) Impulse responce characteristics of secondary path $S(z)$ used in computer simulations, (b) The corresponding magnitude responce characteristics of $S(z)$

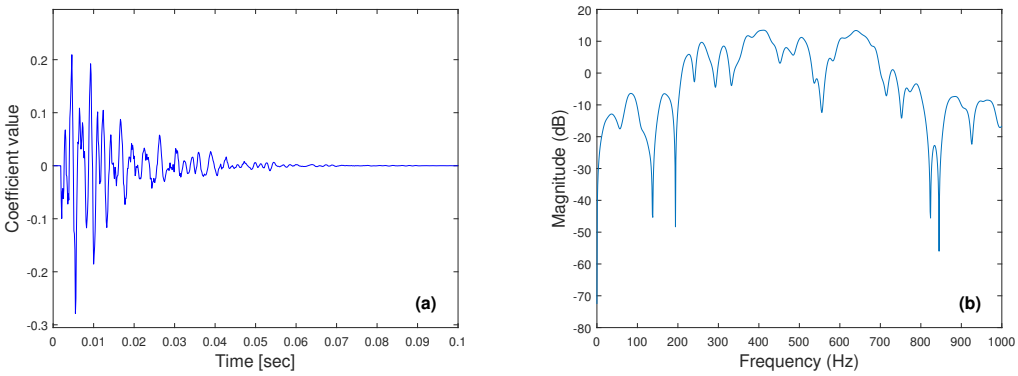

Figure 3.2: (a) Impulse responce characteristics of secondary path $P(z)$ used in computer simulations, (b) The corresponding magnitude responce characteristics of $P(z)$

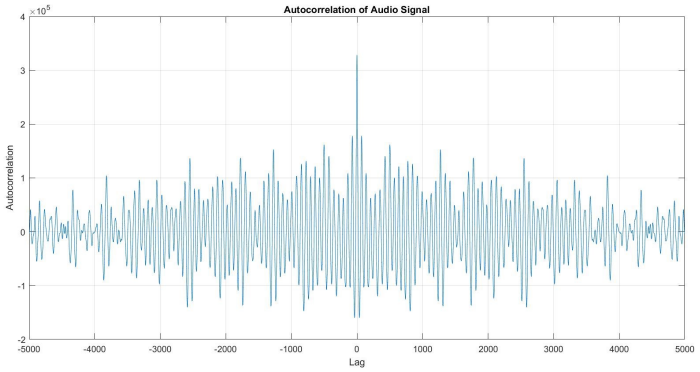

Figure 3.3: Autocorrelation of recorded MRI sound

3.1.2 Periodic nature of MRI Sound

MRI is a medical imaging technique used to visualize the internal structures of the body in detail. MRI machines use strong magnetic fields and radio waves to create images of organs, tissues and other structures inside the body.

Loud noises that occur during an MRI are primarily due to the rapid switching of magnetic fields within the machine. When the magnetic field is turned on and off quickly, it causes the metal coils inside the machine to vibrate, which in turn generates sound waves. Additionally, gradient coils, which are used to create detailed images, make loud tapping or tapping noises when turned on and off to control the magnetic field.

These noises may vary in intensity and frequency throughout the scan depending on the sequence used to acquire the images. Although the sounds can be loud

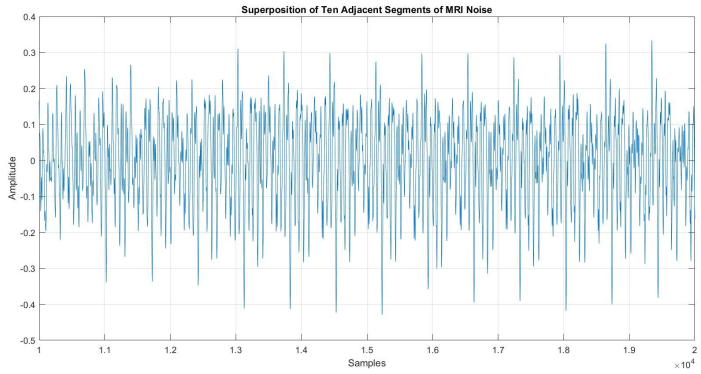

Figure 3.4: Superposition of ten Adjacent Segments of MRI noise

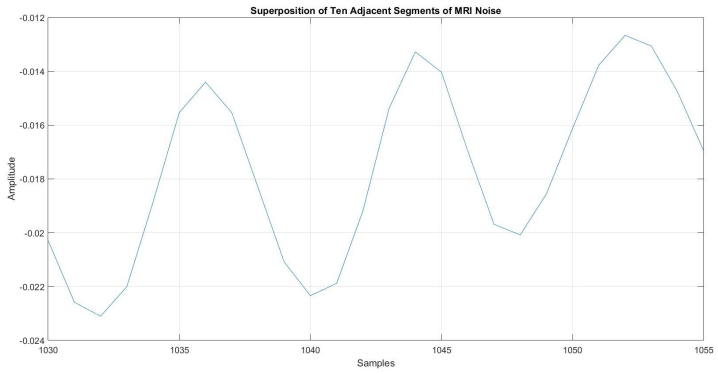

Figure 3.5: Superposition of ten Adjacent Segments of MRI noise for 30 samples

and sometimes disturbing to patients. To reduce discomfort, patients are often given earplugs or headphones to help block out noise. The noise gererated by MRI exhibits quasi periodic nature. The periodic nature of fMRI acoustic noise is primarily explained by the repetitive current levels of the gradient coils. The use of linear predictive modeling facilitates efficient sequential noise removal. The duration of each sample corresponds to the main period of the reference signal. This quasi-periodic characteristic is evident from autocorrelation analysis of recorded fMRI audio taken from the open sourse MRI sound from the Children's hospital of Philadelphia as shown in Fig. 3.3, where repeating patterns indicate a nearly periodic nature of the signal. Fig. 3.4 further explains this concept by overlaying the signals, showing how they are aligned. A zoomed version of Fig. 3.5 clearly illustrates the overlapping waveforms, providing clear evidence of their periodicity.

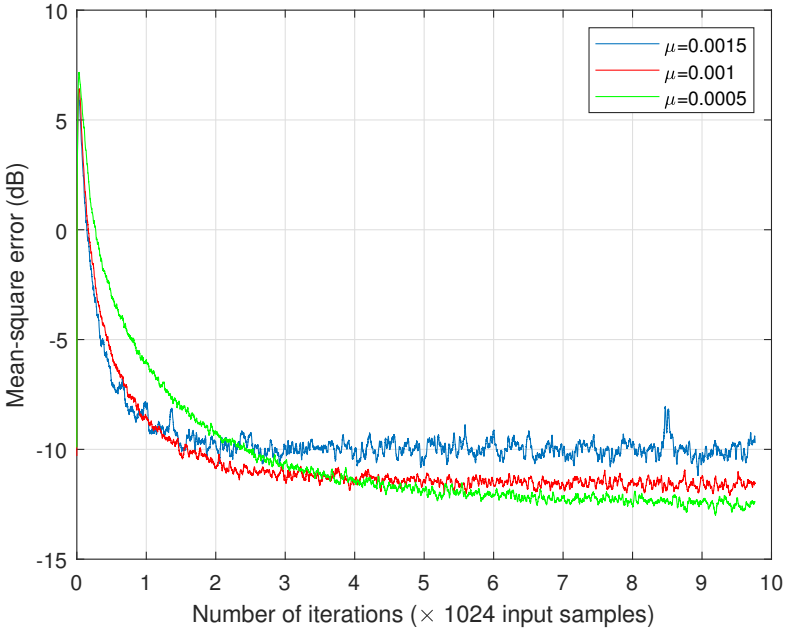

Figure 3.6: MSE curve for different step-size parameters

Table 3.1: Simulation Parameters for FxLMS algorithm

Algorithm	FxLMS			
Acoustic Paths and Adaptive Filters length				
FIR Filter	$P(z)$	$S(z)$	$W(z)$	$S'(z)$
Filter Length	128	64	64	64
Step-Size Parameter	μ=0.001			
Realizations	200			

3.1.3 Effect of Step-size paramater

The simulations for different step-sizes using FxLMS were done to compare the performance in terms of the steady-state performance and convergence rate. As an input the broadband noise from 20Hz-2000 Hz was simulated at 8 kHz sampling frequency. Mean Squared Error (MSE) is the most commonly used metric used to compare the algorithms and its parameters. It is often employed as a metric to evaluate how well an ANC algorithm is performing in minimizing the difference between the desired signal and the estimated signal. The parameters used for simulations are given in Table 3.1. The corresponding graphs for step-sizes of 0.0005, 0.001 and 0.0015 in terms of the MSE are given in Fig. 3.6. As can be observed in Fig. 3.6, increasing the step-size leads to a reduction in the time

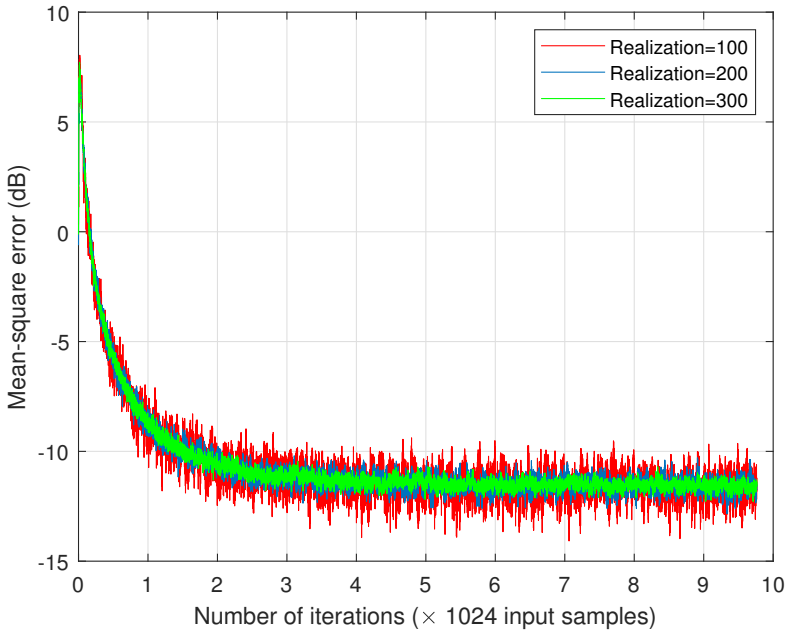

Figure 3.7: MSE curve for different realization numbers

required for convergence, however it shows poor steady-state performance compared to the smaller step-size paramater. Such observations highlight the complex trade off between convergence speed and steady-state stability, which is key to the optimization and control of dynamic systems.

3.1.4 Effect of Realization Number

The simulations include a range of realization numbers to study the impact on the performance of the algorithms. The FxLMS algorithm was tuned with a step size of 0.001, and the broadband signal ranging from 20 Hz to 2000 Hz was simulated as input. Three separate MSE curves were plotted corresponding to realization numbers of 100, 200, and 300 in Fig. 3.7, that facilitate a comprehensive analysis of the performance of algorithms at different realization numbers. The following obervations were made: a higher realization number corresponds to reduced errors and improved convergence to optimal solutions with less fluctuations. The main disadvantage of using a large number of realizations is the increased computational complexity and resource requirements. Processing more realizations requires more memory resulting in longer simulation times and higher computational costs. Thus, while more realizations can provide more accurate estimates and better algorithmic performance, this often comes at the cost of increased com-

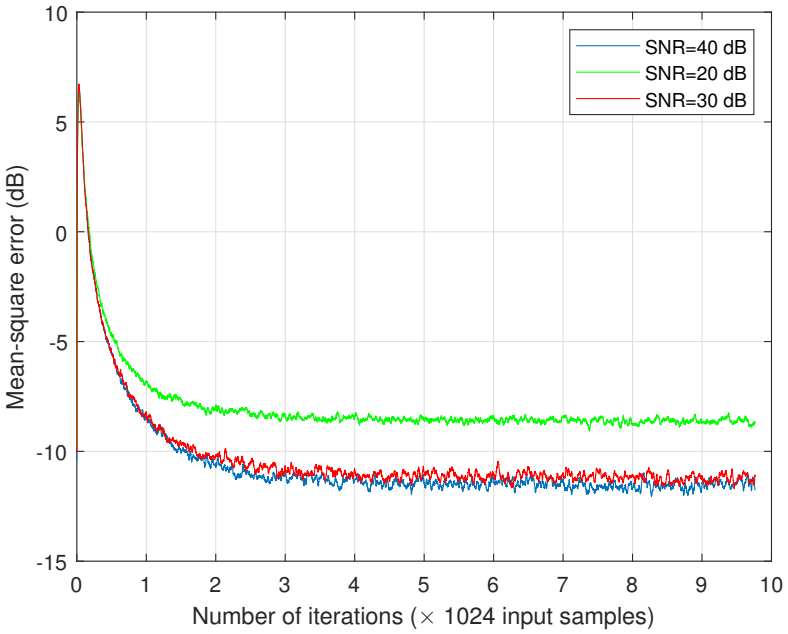

Figure 3.8: MSE curve for different SNR values

putational cost. Achieving a balance between accuracy and computational efficiency is important when determining the appropriate number of realization for a given application.

3.1.5 Effect of Noise Variance

The noise variance is an important factor to consider when comparing the performance of algorithms. With the increase of variance of the input noise, the complexity of the system also increases, leading to challenges for adaptive algorithms to efficiently adapt and reduce noise. Therefore, higher levels of noise variance may result in poor performance in terms of convergence rate, steady-state error, and overall algorithmic stability and robustness.

In practical applications, high level of noise introduce greater uncertainty and randomness into the system, making it more difficult for algorithms to distinguish between the desired signal and the noise. This can lead to increased difficulty in accurately estimating system parameters and adapting algorithm coefficients to achieve higher performance.

Simulations were run with signal-to-noise ratio (SNR) levels, specifically SNR values of 20, 30, and 40. These SNR paramtes represent different levels of noise relative to the extent of the original MRI noise. By evaluating the algorithm's

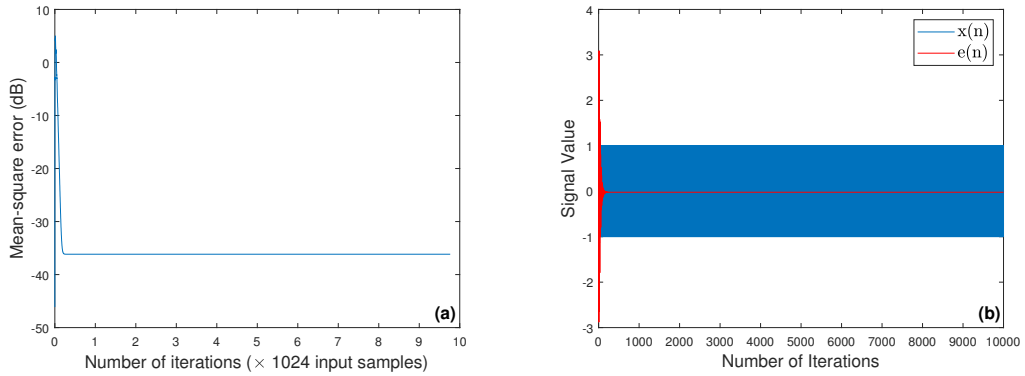

Figure 3.9: (a) MSE curve versus number of iterations for tonal signal, (b) Tonal signal $x(n)$ and error signal $e(n)$ versus number of iterations

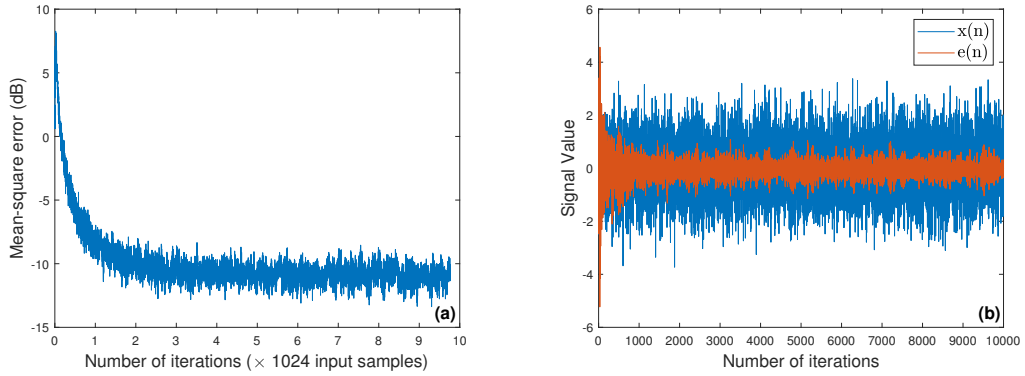

Figure 3.10: (a) MSE curve versus number of iterations for broadband bandlimitted signal, (b) Broadband bandlimitted signal $x(n)$ and error signal $e(n)$ versus number of iterations

performance under different SNR conditions, it can be observed that noise variance affects system behavior.

Higher SNR values indicate a stronger signal compared to background noise. As it can be shown in Fig. 3.8, the higher SNR values result in smaller difference between the output and desired signal.

3.1.6 Experimental Results for FxLMS

To test the FxLMS algorithm, various signals that include tonal noise, broadband noise and recorded MRI sound are selected as the input.

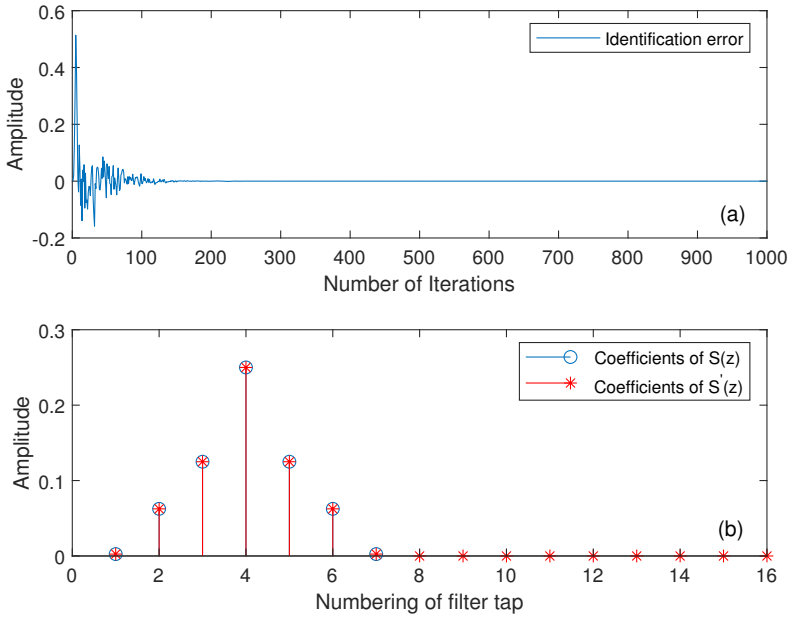

Figure 3.11: a) Identification error of Secondary Path modelling b) Coeficients of true and estimated secondary paths

Case I: Tonal Signal

Tonal Signal at frequency of 1 kHz was used as a reference signal. White Gaussian noise with zero-mean at SNR of 40 dB was added. The MSE curve for 10000 iterations over 200 realizations is illustrated in Fig. 3.9a. Based on the curve MSE is converged to 35 dB. Input signal and residual error after operation of ANC are demonstrated in Fig. 3.9b. After approximately 700 iterations the residual error is converging to zero.

Case II: Broadband Bandlimitted Signal

The broadband bandlimitted signal within the frequency range of 100-2000 Hz was simulated as the application of ANC system is dedicated for MRI sound in low frequency range. The same white noise at 40 dB as in case I was added. The similar performance can be observed in Fig. 3.10, however MSE for this case is at aroung 15 dB. This can be explained by the fact that the handling tonal noises is much more easier compared to the broadband as the ANC system parameters can be tuned specifically for the particular frequency.

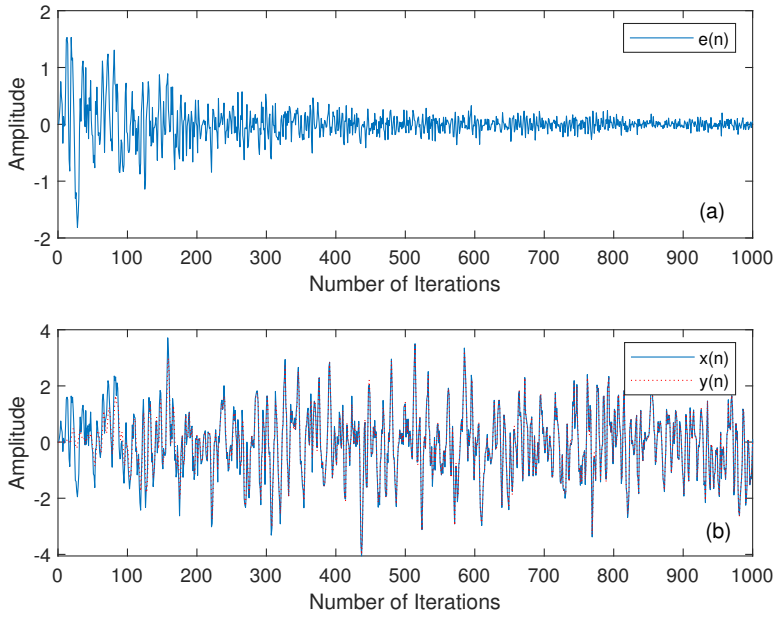

Figure 3.12: (a) error signal $e(n)$ versus number of iterations for broadband bandlimitted reference signal (b) Input signal $x(n)$ and output signal $y(n)$ versus number of iteration for broadband bandlimitted reference signal

3.2 Simulations for Online Secondary Path Modelling techniques

Errikson's method

Computer simulations using MATLAB have been employed to analyze methods' performance. The impulse response of the computer-generated secondary path is within the frequency range of 100 to 2000 Hz with a filter duration set to 0.1 seconds. The length 16 of tap-weight was used for $S(z)$. The primary path used for the

Table 3.2: Simulation Parameters for Secondary Path Modelling

Acoustic Paths and Adaptive Filters length				
FIR Filter	$P(z)$	$S(z)$	$W(z)$	$S'(z)$
Filter Length	256	128	128	128
Step-Size Parameters				
Errikson's method	μ_w=0.01 μ_s=0.001			
Akhtar's method	μ_w=0.01 $\mu_{s_{\min}}$=0.001 $\mu_{s_{\max}}$=0.1			

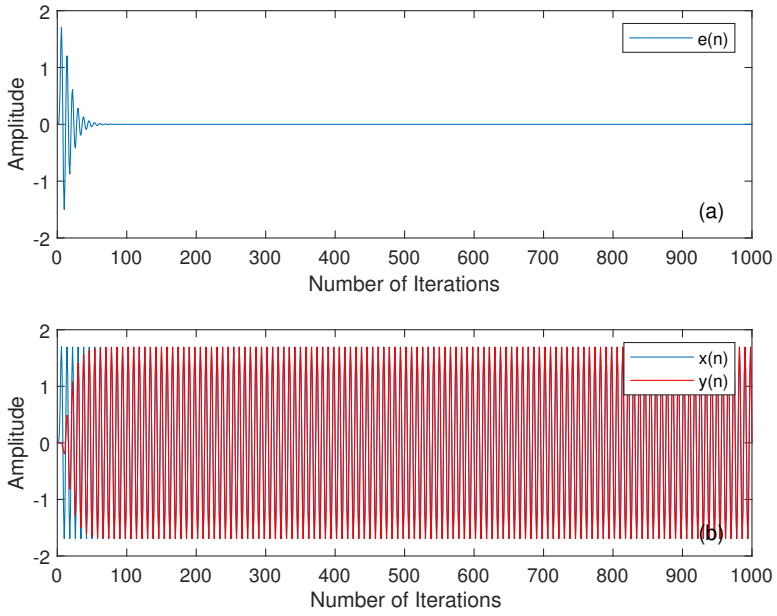

Figure 3.13: (a) error signal $e(n)$ versus number of iterations for tonal reference signal using Errikson's method (b) Input signal $x(n)$ and output signal $y(n)$ versus number of iteration for tonal reference signal using Errikson's method

experiment was computer simulated with filter length of 0.1 seconds. The Errikson's method with the use of the auxilliary noise was simiulated. Identification error, which is the difference between the true secondary path and its estimation is depicted in Fig. 3.11a, and Fig. 3.11b shows the coefficients of the secondary path filter $S(z)$ and secondary path estimation filter $S'(z)$. As it can be seen the error gradually converges towards negligible levels, approaching zero, and the coefficients are equalized suggesting successful adaptation and convergence of the estimation of secondary path. The Errikson's method was tested for two different cases of input signal: broadband bandlimitted signal and tonal signal.

The reference signal used for this simulation is broadband random signal of 20-2000 Hz. A noise with Signal-to-Noise Ratio (SNR) of 40 dB was added to this input signal. The resulting performance of the algorithm is depicted in Fig. 3.12. based on the input, output and residual error.

A tonal signal with a frequency of 1kHz was used as a reference signal. A zero-mean white Gaussian noise of 40 SNR is also added. Fig. 3.13. shows the input and output signal, and corresponding residual error.

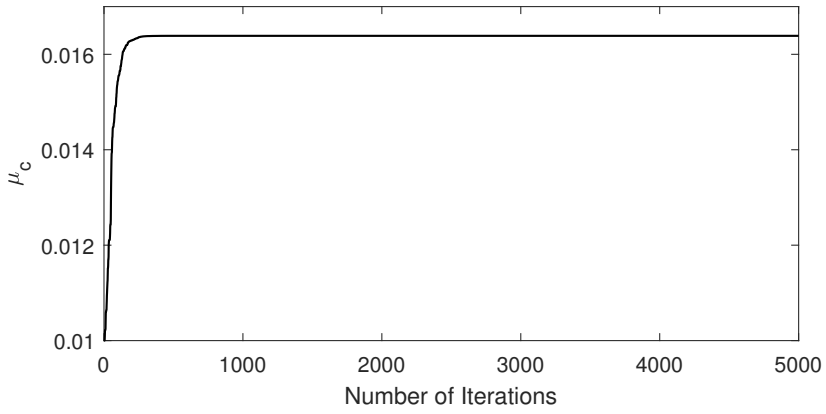

Figure 3.14: Step-Size adapatation for Akhtar's method

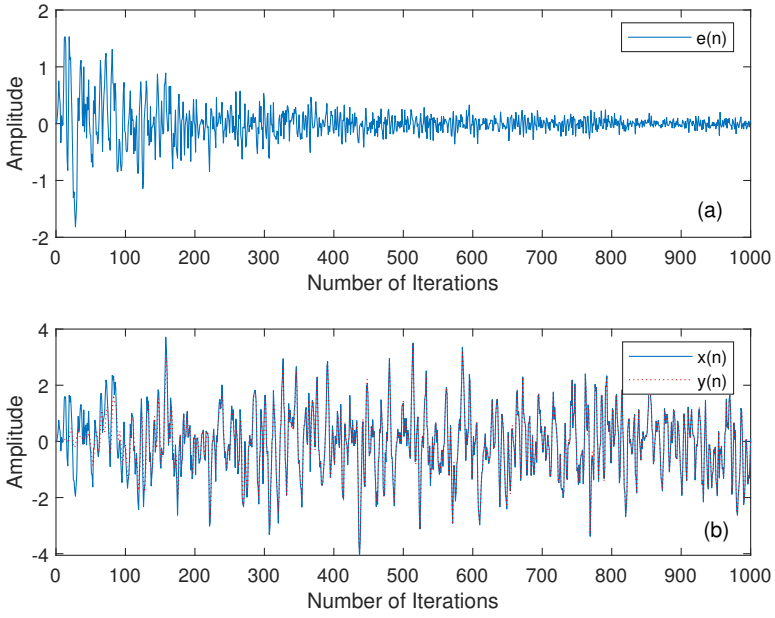

Figure 3.15: (a) error signal $e(n)$ versus number of iterations for broadband bandlimitted reference signal using Akhtar's method (b) Input signal $x(n)$ and output signal $y(n)$ versus number of iteration for broadband bandlimitted reference signal using Akhtar's method

Akhtar's method

The simulations were done for method proposed by Akhtar. The same computer simulated primary and secondary path were used. The simulation parameters are given in Table 3.2. The adaptation of modelling filter step-size can be shown in Fig.

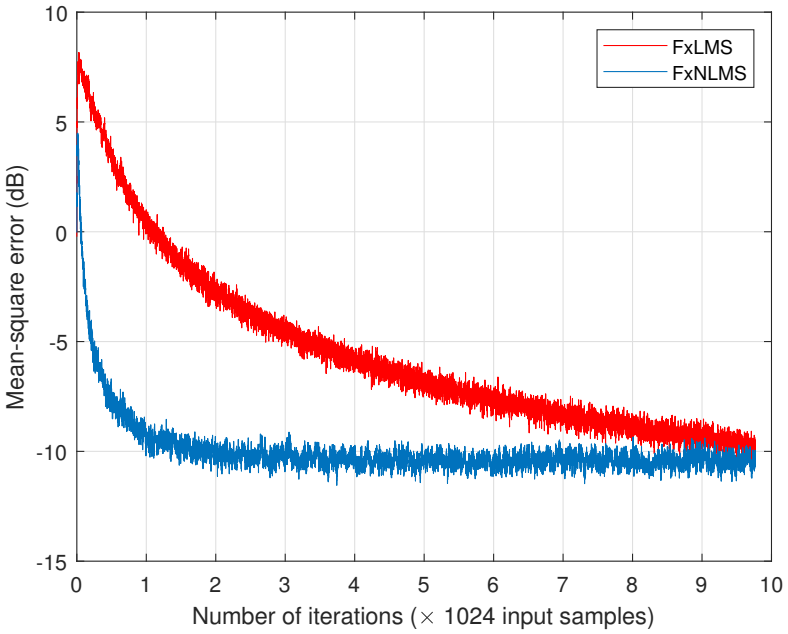

Figure 3.16: MSE curves for FxLMS and FxNLMS algorithms based ANC system

3.14. The step-size limits were determined such that the adaptation was not too slow or very fast with large errors. In the beginning the small step size was used, and then step-size will be decreased when the disturbance signal is minimized. The resulting error signal of ANC system is illustrated in Fig. 3.15, and the curve is approaching to 0.

3.3 Performance Comparisons of Benchmark Algorithms

3.3.1 FxNLMS algorithm simulations

ANC system with FxNLMS alorithm was simulated. The same parameters were used described in Table 3.2. The main difference with FxLMS algorithm in its step-siize that changes depending on the power of the input signal, making overall system more stable. Fig. 3.16 demonstrates the performance of FxNLMS algorithm compared to FxLMS based on the MSE curve.

3.3.2 FxVSSLMS algorithm simulations

The ANC system benchmark algorithm with variable step-size is implemented, and the following formulas was used for adaptation of the step-size parameter for

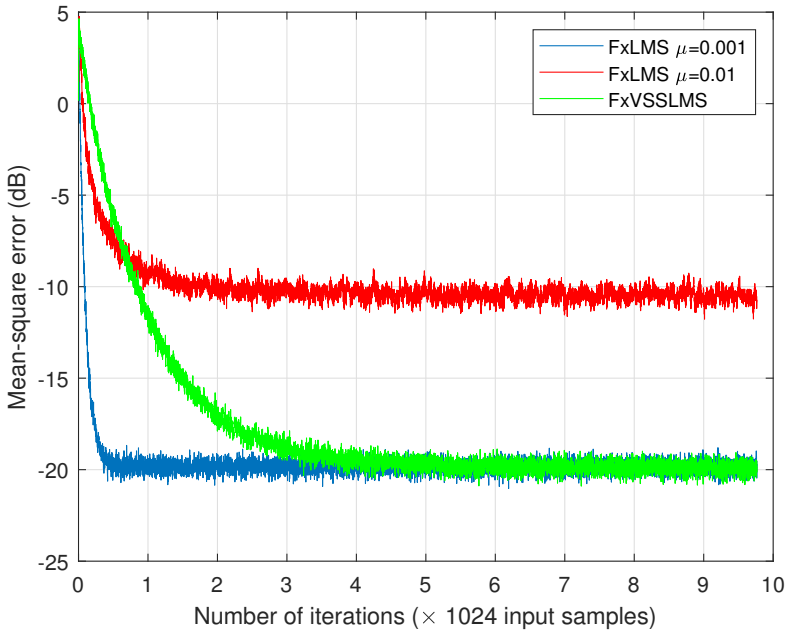

Figure 3.17: MSE curves for FxVSSLMS and FxLMS algorithms based ANC system

each iteration:

$$\mu(n+1) = \alpha\mu(n) + \gamma e(n)^2 \tag{3.1}$$

with parameters: α=0.95 and γ=0.01. To ensure stability of the system upper and lower boundaries of step-size were determined by trial-and-error : μ_{min}=0.0001 μ_{max}=0.01. Two ANC processes with FxLMS algorithm at two different values of step-size were simulated in order to compare the operation of FxVSSLMS based ANC system. The MSE curves for this process is illustrated in Fig. 3.17. As it can be shown the FxVSSLMS algorithm converges faste compared to the FxLMS algorithm with small step-size, and shows better steady-state performance than FxLMS algorithm with large step-size. This concludes that the FxVSSLMS algorithm provides the opportunity to solve the trade off between these mentioned two performance measures. However, FxVSSLMS algorithm requires higher computational complexity due to the derrivation of step-size depending on the filter length.

3.3.3 Quantative Results

The total amount of noise cancelation is shown in Table 3.3 in terms of noise attenuation level (NAL) in dB. NAL is calculated using the following formula [32]:

Table 3.3: NAL values for adaptive algorithms

Input Signal	Input Signal Frequencies (Hz)	NAL in dB			
		SNR	FxLMS	FxNLMS	FxVSSLMS
Multitonal noise	1k, 1.1k, 1.2k, 1.3k, 1.4k, 1.5k	40	32.4371	36.5353	37.4122
Broadband	20-2000	40	17.6783	18.8712	22.1267
Bandlimitted	200-300	40	18.7071	19.2201	17.0342
Recorded MRI sound	10-2000	40	14.3021	15.1231	19.4256

$$\text{NAL(dB)} = 10\log\left[\frac{|(x_c(n))|^2}{|(e_c(n))|^2}\right] \tag{3.2}$$

where: $|(x_c(n)|)^2$ represents the power of the noise signal, and $|(e_c(n)|)^2$ represents the power of the error signal after converging, after about 5000 iterations.

The ANC system show better performance in terms of the NAL for narrowband signal compared to the broadband bandlimitted signal due to the concentrated energy within limited frequency ranges. Narrowband signals allow for more precise identification and cancellation of specific frequencies, enabling the ANC system to achieve more effective noise reduction.In contrast, the broader frequency spectrum of broadband signals can pose challenges in accurately and comprehensively canceling noise. Choosing amongst these methods requires weighing convergence speed, stability, and error signal optimization carefully, emphasizing the complex decision-making process in adaptive filtering applications.

Chapter 4

Conclusion

4.1 Summary of Work Done

In conclusion, this study has provided a comprehensive understanding of ANC and its operational mechanisms. Through an deep literature review, ANC based on the current fundamental adaptive algorithms and their diverse variations were implemented and simulated. The respective strengths and limitations were shown through simulations for different cases were concluded. Furthermore, an analysis of the benchmark algorithm's performance metrics, including computational complexity, steady-state performance, and convergence rate has been conducted demonstarting information into its efficiency and feasibility in real-world applications. Additionally, by utlizing the performance metrics across various reference signals, the adaptability and robustness of ANC systemswere tested under diverse conditions. Lastly, through the detailed analysis of noise generated by MRI systems, this study has demonstrated the feasibility and potential application of the implemented ANC system in mitigating unwanted noise, contributing to the advancement of noise control technologies.

4.2 Future work

It is anticipated on acquiring deeper knowledge and reproduce the results of the state of the art in the ANC system particularly in the context of reducing noise generated by MRI machines. Signal decomposition technique was studied, and the possible efficiency was offered for integrating into ANC system. Therefore, elaborating into the decomposition techniques could be done. As part of future work, a focused effort will be directed towards further studying and including additional existing benchmark algorithms for a more comprehensive comparison and evaluation of their performance by various metrics. Moreover, an important aspect of future research will involve the analysis, modification, and development of new

algorithms implemented with specific requirements and challenges encountered in ANC applications, particularly in MRI noise reduction. Therefore, it is expected that novel solutions can be proposed to address the current issues of noise control system in complex environments.

Bibliography

[1] C. H. Hansen and K. L. Hansen, *Noise control: from concept to application*. CRC Press, 2021.

[2] H. M. Lee, Y. Hua, Z. Wang, K. M. Lim, and H. P. Lee, "A review of the application of active noise control technologies on windows: Challenges and limitations," *Applied Acoustics*, vol. 174, p. 107 753, 2021.

[3] T. Yamashiro, K. Morita, and K. Nakajima, "Evaluation of magnetic resonance imaging acoustic noise reduction technology by magnetic gradient waveform control," *Magnetic Resonance Imaging*, vol. 63, pp. 170–177, 2019.

[4] D. Shi, W.-S. Gan, J. He, and B. Lam, "Practical implementation of multichannel filtered-x least mean square algorithm based on the multiple-parallel-branch with folding architecture for large-scale active noise control," *IEEE Transactions on Very Large Scale Integration (VLSI) Systems*, vol. 28, no. 4, pp. 940–953, 2019.

[5] A Krishna, L Ravinchandra, T. K. Fei, and L. C. Yong, "Active noise reduction using lms and fxlms algorithms," vol. 1228, no. 1, p. 012 064, 2019.

[6] M. J. McJury, "Acoustic noise and magnetic resonance imaging: A narrative/descriptive review," *Journal of Magnetic Resonance Imaging*, vol. 55, no. 2, pp. 337–346, 2022.

[7] N. Lee, Y. Park, and G. W. Lee, "Frequency-domain active noise control for magnetic resonance imaging acoustic noise," *Applied Acoustics*, vol. 118, pp. 30–38, 2017.

[8] Kuo, *Active Noise Control Systems: Algorithms and DSP Implementations*. Wiley, 1996.

[9] B. K. Pancholi and P. S. Modi, "Noise reduction in clinical mri scans employing filter combining techniques," in *2022 2nd International Conference on Technological Advancements in Computational Sciences (ICTACS)*, 2022, pp. 474–480.

[10] G. Kannan, A. A. Milani, I. M. Panahi, and R. W. Briggs, "An efficient feedback active noise control algorithm based on reduced-order linear predictive modeling of fmri acoustic noise," *IEEE transactions on Biomedical Engineering*, vol. 58, no. 12, pp. 3303–3309, 2010.

[11] Z. Zhang, S. Chen, Z. Zhou, and H. Li, "An active noise control system based on reference signal decomposition," *Digital Signal Processing*, vol. 129, p. 103 676, 2022.

[12] G. Kannan, A. A. Milani, I. Panahi, and R. Briggs, "Equalizing secondary path effects using the periodicity of fmri acoustic noise," in *2008 30th Annual International Conference of the IEEE Engineering in Medicine and Biology Society*, IEEE, 2008, pp. 25–28.

[13] A. Ganguly, S. H. K. Vemuri, and I. Panahi, "Parallel feedback active noise control of mri acoustic noise with signal decomposition using hybrid rls-nlms adaptive algorithms," in *2014 36th Annual International Conference of the IEEE Engineering in Medicine and Biology Society*, IEEE, 2014, pp. 3220–3223.

[14] F. Yang, J. Guo, and J. Yang, "Stochastic analysis of the filtered-x lms algorithm for active noise control," *IEEE/ACM Transactions on Audio, Speech, and Language Processing*, vol. 28, pp. 2252–2266, 2020.

[15] S. Kuo and W.-S. Gan, "Active noise control systems with optimized secondary path," vol. 1, Oct. 2004, 765 –770 Vol.1, ISBN: 0-7803-8633-7. DOI: 10.1109/CCA.2004.1387306.

[16] H. Meng and S. Chen, "A modified adaptive weight-constrained fxlms algorithm for feedforward active noise control systems," *Applied Acoustics*, vol. 164, p. 107 227, 2020.

[17] M. T. Akhtar and W. Mitsuhashi, "Improved adaptive algorithm for active noise control of impulsive noise," in *2008 51st Midwest Symposium on Circuits and Systems*, IEEE, 2008, pp. 330–333.

[18] S.-C. Chan and Y. Chu, "Performance analysis and design of fxlms algorithm in broadband anc system with online secondary-path modeling," *IEEE transactions on audio, speech, and language processing*, vol. 20, no. 3, pp. 982–993, 2011.

[19] S. Li, S. Wu, Y. Wang, W. Guo, and Y. Zhou, "An improved nlms algorithm based on speech enhancement," in *2015 IEEE Advanced Information Technology, Electronic and Automation Control Conference (IAEAC)*, IEEE, 2015, pp. 896–899.

[20] J. Zhang, H. Sun, P. N. Samarasinghe, and T. D. Abhayapala, "Active noise control over multiple regions: Performance analysis," in *ICASSP 2020-2020 IEEE International Conference on Acoustics, Speech and Signal Processing (ICASSP)*, IEEE, 2020, pp. 8409–8413.

[21] S. Tian, W. Wang, and L. Cheng, "An improved strategy for the variable step-size lms algorithm," *International Journal of Simulation–Systems, Science & Technology*, vol. 17, no. 8, 2016.

[22] S. D. Snyder and C. H. Hansen, "The effect of transfer function estimation errors on the filtered-x lms algorithm," *IEEE Transactions on Signal Processing*, vol. 42, no. 4, pp. 950–953, 1994.

[23] S. M. Kuo and D. Vijayan, "A secondary path modeling technique for active noise control systems," *IEEE Transactions on Speech and Audio Processing*, vol. 5, no. 4, pp. 374–377, 1997.

[24] C. Bao, "Comparison of two on-line identification algorithms for active noise control," in *Recent advances in active control of sound and vibration*, 1993.

[25] L. J. Eriksson and M. C. Allie, "Use of random noise for on-line transducer modeling in an adaptive active attenuation system," *The Journal of the Acoustical Society of America*, vol. 85, no. 2, pp. 797–802, 1989.

[26] M. T. Akhtar, M. Abe, and M. Kawamata, "A new variable step size lms algorithm-based method for improved online secondary path modeling in active noise control systems," *IEEE Transactions on Audio, Speech, and Language Processing*, vol. 14, no. 2, pp. 720–726, 2006.

[27] Y. Ma and Y. Xiao, "A new strategy for online secondary-path modeling of narrowband active noise control," *IEEE/ACM Transactions on Audio, Speech, and Language Processing*, vol. 25, no. 2, pp. 420–434, 2016.

[28] A. Carini and S. Malatini, "Optimal variable step-size nlms algorithms with auxiliary noise power scheduling for feedforward active noise control," *IEEE transactions on audio, speech, and language processing*, vol. 16, no. 8, pp. 1383–1395, 2008.

[29] D. Yang, D. Song, X. Zeng, X. Wang, and X. Zhang, "Adaptive nonlinear anc system based on time-domain signal reconstruction technology," *Mechanical Systems and Signal Processing*, vol. 162, p. 108 056, 2022.

[30] J. G. Proakis, *Digital signal processing: principles, algorithms, and applications, 4/E*. Pearson Education India, 2007.

[31] R. M. Reddy, I. M. Panahi, and R. Briggs, "Hybrid fxrls-fxnlms adaptive algorithm for active noise control in fmri application," *IEEE Transactions on Control Systems Technology*, vol. 19, no. 2, pp. 474–480, 2010.

[32] M. W. Munir and W. H. Abdulla, "On fxlms scheme for active noise control at remote location," *IEEE Access*, vol. 8, pp. 214 071–214 086, 2020.